Kinetic and Mechanistic Studies on the Hydrolysis of Ubiquitin C-Terminal 7-Amido-4-Methylcoumarin by Deubiquitinating Enzymes

Luan C. Dang, Francesco D. Melandri, and Ross L. Stein*

ProScript, Inc., 38 Sidney Street, Cambridge, Massachusetts 02139

Received September 22, 1997; Revised Manuscript Received December 9, 1997

ABSTRACT: Deubiquitinating enzymes constitute a family of cysteine hydrolases that specifically cleave ubiquitin-derived substrates of general structure Ub-X, where X can be any number of leaving groups ranging from small thiols and amines to Ub and other proteins (Ub, ubiquitin). We have developed a general assay for deubiquitinating enzymes based on the substrate ubiquitin C-terminal 7-amido-4-methylcoumarin (Ub-AMC). Ub-AMC is efficiently hydrolyzed with liberation of highly fluorescent AMC by two rabbit reticulocyte deubiquitinating enzymes: isopeptidase T (IPaseT), a member of the gene family of ubiquitin-specific processing enzymes, and UCH-L3, a member of the family of ubiquitin C-terminal hydrolases. We used this new assay to probe kinetic and mechanistic aspects of catalysis by IPaseT and UCH-L3. Results from four series of experiments are discussed: (1) For UCH-L3, we determined steady-state kinetic parameters that suggest a diffusion-limited reaction of UCH-L3 with Ub-AMC. To probe this, we determined the viscosity dependence of k_c/K_m, as well as k_c. We found complex viscosity dependencies and interpreted these in the context of a model in which association and acylation are viscosity-dependent but deacylation is viscosity-independent. (2) The kinetics of inhibition of UCH-L3 by ubiquitin C-terminal aldehyde (Ub-H) were determined and reveal a K_i that is less than 10^{-14} M. Several mechanims are considered to account for the extreme inhibition. (3) The IPaseT-catalyzed hydrolysis of Ub-AMC is modulated by Ub with activation at low [Ub] and inhibition at high [Ub]. (4) Finally, we compare k_c/K_m values for deubiquitinating enzyme-catalyzed hydrolysis of Ub-AMC and Z-Leu-Arg-Gly-Gly-AMC. For IPaseT, the ratio of rate constants is 10^4, while for UCH-L3 this ratio is $>10^7$. These results suggest the following: (i) Deubiquitinating enzymes are able to utilize the free energy that is released from remote interactions with Ub-containing substrates for stabilization of catalytic transition states, and (ii) UCHs are more efficient at utilizing the energy from these interactions, presumably because they do not possess a binding domain for a Ub "leaving group".

The ubiquitin−proteasome pathway is the cell's principle mechanism for protein catabolism and has both housekeeping roles and roles in the turnover of many regulatory proteins (*1*−*5*). Proteins that are destined to be degraded through the ubiquitin−proteasome pathway are first covalently tagged with a molecule of ubiquitin, a 8.6-kDa heat-stable protein. This tagging reaction involves three sequential enzyme-catalyzed reactions that ultimately ligate the C-terminal Gly of Ub[1] onto ϵ-amines of Lys residues on the substrate protein. A polyUb chain is then elaborated on the protein through the ligation of additional monomers of Ub in successive rounds of ubiquitination. These Ub molecules are added to specific Lys residues of the proximal Ub of the propagating polyUb chain. Proteins with long polyUb chains are recognized by the 26S proteasome complex for proteolytic degradation and recycling of intact Ub monomers (*4*, *6*, *7*). Alternately, the polyubiquitinated protein will be subject to the action of certain deubiquitinating enzymes to generate Ub monomers.

Deubiquitinating enzymes (*4*, *7*−*9*) constitute a large family of cysteine hydrolases that specifically cleave ubiquitin-derived substrates of the general structure Ub^{1-72}-Leu^{73}-Arg^{74}-Gly^{75}-Gly^{76}-X, where X can be any number of leaving groups ranging from small thiols and amines to Ub and other proteins. Recently, important biological roles have been discovered for many members of this family. For example, the human *Unph* gene encodes a deubiquitinating enzyme whose overexpression leads to oncogenic transformation of NIH3T3 cells (*10*); *tre-2* oncogene is structurally related to *Unph* and also encodes a deubiquitinating enzyme (*11*); DUBs are a subfamily of cytokine-inducible, immediate−early genes that encode a deubiquitinating enzyme with growth regulatory activities (*12*); UCH-L1 is involved not only in neural development (*13*) but also in the differentiation of a lymphoblastic leukemia cell line, Reh (*14*); and the *Drosophilia fat facets* gene encodes a deubiquitinating enzyme which is required for eye development in the fly (*15*).

These enzymes also differ widely in their size. High-molecular-weight deubiquitinating enzymes (∼100 000) hy-

* To whom correspondence should be addressed.

[1] Abbreviations: AMC, 7-amido-4-methylcoumarin; DTT, dithiothreitol; FI, fluorescence intensity; IPaseT, isopeptidase T.; polyUb, polyubiquitin chains formed through isopeptide linkages of Gly^{76} of one Ub and the ϵ-amine of Lys^{48} of another Ub; Ub, ubiquitin; Ub-H, ubiquitin aldehyde; Ub-AMC, ubiquitin C-terminal 7-amido-4-methylcoumarin (i.e., Ub^{1-72}-Leu^{73}-Arg^{74}-Gly^{75}-Gly^{76}-AMC); Ub-H, ubiquitin C-terminal aldehyde (i.e., Ub^{1-72}-Leu^{73}-Arg^{74}-Gly^{75}-Gly^{76}-H); UBP, ubiquitin-specific processing enzyme; UCH, ubiquitin C-terminal hydrolases.

S0006-2960(97)02336-2 CCC: $15.00
Published on Web 01/30/1998

Scheme 1: Minimal Mechanism for UCH-L3-Catalyzed Hydrolysis of Ub-AMC

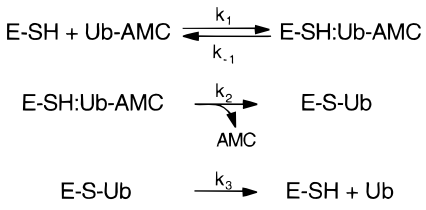

drolyze Ub^{1-72}-Leu^{73}-Arg^{74}-Gly^{75}-Gly^{76}-X derivatives, where X is a protein or another molecule of Ub. These enzymes are known as ubiquitin-specific processing enzymes (UBPs) and are thought to have domains adjacent to the primary Ub−substrate binding site that can recognize and bind these proteinacious leaving groups. The most thoroughly UBP is isopeptidase T (*6, 7, 9, 16, 17*), which cleaves substrates where X is Ub (*7*). In contrast, low-molecular-weight deubiquitinating enzymes (∼30 000) hydrolyze Ub derivatives where X is a thiol or amine and are thought not to possess a binding domain for protein leaving groups (*8, 11, 18*−*20*). These enzymes are known as ubiquitin C-terminal hydrolases (UCHs).

Despite these differences in physiologic role and size, all deubiquitinating enzymes appear to hydrolyze their substrates through a common chemical mechanism (Scheme 1) involving the binding of Ub^{1-72}-Leu^{73}-Arg^{74}-Gly^{75}-Gly^{76}-X, nucleophilic attack of the thiol moiety of the active site Cys residue on the carbonyl carbon of Gly^{76}, formation of an acyl-enzyme intermediate, Ub^{1-75}-$NHCH_2C(O)S$−E, and hydrolysis of this intermediate to liberate free enzyme and Ub.

It has been possible to exploit this common mechanism to design a substrate, Ub-OEt, that is hydrolyzed by all deubiquitinating enzymes (*8, 20*). Assays that use this substrate are HPLC-based and lack sensitivity, precision, and convenience. However, we reasoned that an assay based on hydrolysis of Ub-AMC might be a better alternative to the former assay. Hydrolysis of the fluorogenic substrate Ub-AMC could be followed continuously and should be exceedingly sensitive and precise. In this paper, we report the preparation of Ub-AMC and that it is efficiently hydrolyzed by both a UBP, isopeptidase T, and a 30-kDa UCH, UCH-L3. We also report features of the mechanism of hydrolysis of Ub-AMC by these enzymes.

EXPERIMENTAL SECTION

General. Buffer salts, bovine Ub, and TPCK-treated bovine trypsin were purchased from Sigma Chemical Co. (St. Louis, MO). Gly-Gly-AMC was obtained from Bachem (King of Prussia, PA). Z-Leu-Arg-Gly-Gly-H was prepared by SynPep, Inc. (Dublin, CA). Ub-H was prepared as previously described (*17*).

Purification of Ubiquitin C−*Terminal Hydrolases.* IPaseT and UCH-L3 were purified to near homogeneity from rabbit reticulocytes as previously reported (*9, 16, 18, 21*). Briefly, rabbit reticulocytes from 700 mL of rich whole blood were washed with cold PBS, lysed in lysis buffer (50 mM HEPES pH 7.6, 10 mM DTT, 0.5 mM EDTA), and then centrifuged at 100000*g* for 1 h. Collected supernatant was applied to a 300-mL DEAE Sepharose (Pharmacia, Uppsala, Sweden) column preequilibrated with buffer A (50 mM HEPES pH 7.6, 1 mM DTT). After washing with 2.5 column volumes, fraction II was eluted with buffer B (50 mM HEPES pH 7.6, 1 mM DTT, 0.5 M NaCl), concentrated by precipitating with 90% ammonium sulfate, and then dialyzed overnight against 4 L of buffer A. Following dialysis, 2.5 mM MgATP was added for 15 min at room temperature and applied to the ubiquitin-Sepharose affinity column (20 mg of protein/mL of resin) preequilibrated with buffer C (50 mM Tris pH 7.2, 0.2 mM DTT, 2.5 mM MgATP). Ub-Sepharose was washed sequentially with four column volumes of buffer C, then with 1 M KCl, and then with 10 mM DTT. Enzymes of interest were eluted with 50 mM Tris pH 9.0, 0.1 mM EDTA, 5 mM DTT. Fractions were neutralized with a 1:10 volume of 1 M Tris pH 7.2, dialyzed against 4 L of buffer A and then applied to a Mono Q anion exchange (Pharmacia) column. Isopeptidase-T and UCH-L3 coeluted at 250 mM NaCl by a 40-column-volume gradient from 0 to 500 mM NaCl. To separate the two enzymes, the Mono-Q fraction was concentrated using a Centricon (3000 MWCO, Amicon) and applied to a Superdex-200 size-exclusion column (Pharmacia) equilibrated with 50 mM HEPES pH 7.6, 1 mM DTT, 100 mM NaCl. Protein concentrations were determined by the Coomassie-Plus protein assay (Pierce, Rockford, IL). Purity was judged by loading >10 μg of protein on a Coomassie-stained 10% SDS−PAGE.

Preparation of Ub-AMC. Gly-Gly-AMC was dissolved to a final concentration of 25 mM in 200 mM HEPES containing 10% DMSO. The pH of the solution (initially pH 6) was slowly adjusted to 6.9 with 1 N NaOH. Ub and trypsin were added to the Gly-Gly-AMC solution to give final concentrations of 500 and 0.1 μM, respectively. The reaction solution was allowed to incubate at 30 °C for 16 h and quenched by the addition of glacial acetic acid to produce a final 5% (v/v) solution. The reaction solution was then fractionated by reverse-phase chromatography (Vydac C_{18} column, 10 × 250 mm) operating at 2.5 mL/min flow rate using a linear gradient of H_2O/AcCN/TFA with 0.2% AcCN/min. Detection was provided by simultaneous UV absorbance at 205 nm and fluorescence at 425 nm (λ_{ex} = 340 nm). The Ub-AMC was collected and lyophilized for 48 h, dissolved in DMSO, and stored as aliquots at −80 °C.

Mass Spectroscopy of Ub and Ub-AMC. Ubiquitin, the HPLC peak from a mock reaction without trypsin, and the fluorescent peak from a trypsin-containing reaction were collected in glass vials. Samples were briefly concentrated by speed-vac at room temperature for 1 h. Mass of each was determined by electrospray mass spectroscopy (M-Scan, West Chester, PA).

Kinetic Methods. (a) General. In a typical kinetic run, 390 μL of assay buffer (50 mM HEPES, 0.5 mM EDTA, pH 7.5, containing 0.1 mg/mL ovalbumin and 1-mM DTT) was added to a 1 mL fluorescence cuvette and the cuvette placed in the jacketed cell holder of a Hitachi 2000 fluorescence spectrophotometer. Reaction temperature was maintained at 25.0 ± 0.02 °C by a circulating water bath. After the reaction solution had reached thermal equilibrium (∼5 min), 1−10 μL of the stock enzyme solution was added to the cuvette. The reaction solution was incubated an additional 30 min to allow DTT-mediated activation of IPaseT or UCH-L3 before the addition of 10 μL of substrate solution in DMSO. Reaction progress was monitored by the increase in fluorescence emission at 460nm (λ_{ex} = 380 nm)

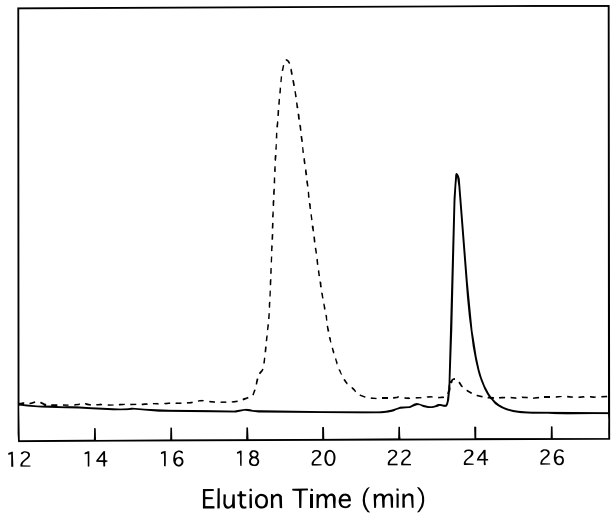

FIGURE 1: Chromatogram for the purification of Ub-AMC. Dashed line corresponds to UV detection at 205 nm, and the solid line corresponds to fluorescence detection (λ_{ex} = 340 nm, λ_{em} = 425 nm). The peaks at 19 and 23.5 min are des-Gly-Gly-Ub and Ub-AMC, respectively.

that accompanies cleavage of AMC from Ub-AMC. For each kinetic run, 200−1000 data points, corresponding to {time, FI} pairs, were collected by a computer interfaced to the fluorescence spectrophotometer.

(b) Titration of UCH-L3 with Ubiquitin Aldehyde. To determine the steady-state dissociation constant for the inhibition of UCH-L3 by Ub-H, we conducted enzyme titration experiments in which residual activity is measured for enzyme reaction solutions in which $[I]_o \sim [E]_o \gg K_i$. Specifically, 2.0-mL reaction solutions containing 10 pM UCH-L3 and various concentrations of Ub-H were allowed to incubate at 25.0 ± 0.02 °C for 4 h. At this end of this time, residual IPaseT activity was measured with Ub-AMC at a final concentration of 50 nM.

(c) Dissociation of the UCH-L3−Ub-H Complex. Enzyme at 50 nM was incubated with 250 nM Ub-H at 25 °C for 24 h in reaction buffer (100 mM HEPES, 10 mM DTT, 0.5 mM EDTA, 0.1 mg/mL ovalbulin). Control sample without Ub-H or sample with Ub-H was then incubated with 20 mM semicarbazide. At time intervals, the UCH-L3/Ub-H/semicarbazide solution was diluted 10-fold into assay buffer containing 500 nM Ub-AMC and the velocity was measured. Similarly, the control UCH-L3/semicarbazide solution was diluted 1000-fold into assay buffer containing 500 nM Ub-AMC and the velocity was measured.

RESULTS

Preparation and Characterization of Ub-AMC. Treatment of an aqueous solution of Ub and Gly-Gly-AMC with trypsin produced a highly fluorescent material with a retention time on reverse-phase HPLC of 23.5 min (see Figure 1). This retention time is longer than the retention time for either Ub (18.5 min; data not shown) or des-Gly^{75}-Gly^{76}-Ub (19 min; Figure 1). Mass spectral analysis of the material that elutes at 23.5 min yields a molecular ion of 8722 Da, which is essentially identical to the calculated mass of 8725 Da for Ub-AMC.[2] Calibration of the experiment was provided by analysis of an authentic sample of Ub, which yielded a mass of 8564 Da, which is identical to its calculated mass of 8568 Da. Estimates of molecular weight for proteins of this size are generally good within 2 or 3 mass units.

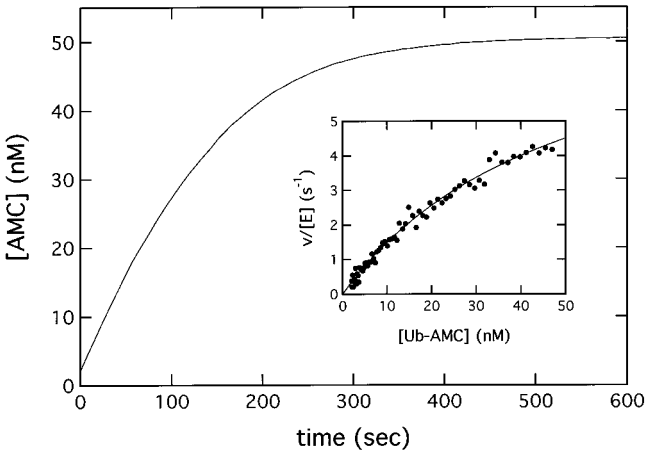

FIGURE 2: Progress curve for the UCH-L3-catalyzed hydrolysis of Ub-AMC. Fluorescence intensity (λ_{em} = 460 nm, λ_{ex} = 380 nm) was recorded for the UCH-L3-catalyzed hydrolysis of Ub-AMC, converted to AMC concentration, and plotted here as a function of time. The reaction was conducted at 25 °C in a pH 7.8 assay buffer containing 50 mM HEPES, 0.5 mM EDTA, 0.1 mg/mL ovalbumin, and 1 mM DTT. In this experiment, the nominal concentrations of UCH-L3 and Ub-AMC were 17.5 pM and 50 nM, respectively. The inset shows a plot of v/[E] vs [Ub-AMC], where v is the instantaneous velocity calculated from the progress curve and [Ub-AMC] is the corresponding substrate concentration. The solid line was drawn using the Michaelis−Menten equation and the following best-fit parameters: k_c = 9.1 ± 0.1 s^{-1} and K_m = (5.1 ± 0.4) × 10^{-8} M.

Additional confirmation that the peak at 23.5 min in Figure 1 is Ub-AMC came from an experiment in which a 50 nM solution of the material was treated with UCH-L3. The assignment of 50 nM was based on a Gly-Gly-AMC fluorescence calibration (λ_{ex} = 340 nm, λ_{em} = 425 nm). As Figure 2 demonstrates, this treatment results in the liberation of 48 nM AMC. This compares favorably with the nominal concentration of Ub-AMC of 50 nM and indicates not only that we have prepared Ub-AMC but that it is in a nativelike conformation that can be recognized by a deubiquitinating enzyme.

Kinetics of UCH-L3-Catalyzed Hydrolysis of Ub-AMC. The experiment of Figure 2 was our first indication that Ub-AMC is an extremely efficient substrate for UCH-L3. In this experiment, complete hydrolysis is achieved in 5 min with an enzyme concentration of only 17.5 pM. A rough estimate of the steady-state parameters can, of course, be obtained from this progress curve. If we apply the method of instantaneous velocities (*22*), we obtain the parameters k_c = 9.1 ± 0.1 s^{-1} and K_m = (51 ± 4) × 10^{-9} M (see inset of Figure 2).

Accurate values of the steady-state kinetic parameters were obtained from initial velocity experiments. At 10 pM UCH-L3, we determined initial velocities as a function of Ub-AMC concentration. The data sets from two independent

[2] If transacylation is conducted under conditions of high trypsin concentration (i.e., >0.5 μM) or extended reaction times (i.e., >30 h), a new fluorescent species is formed with a mass of 8452 Da which corresponds to Ub$^{1-71}$-Arg^{72}-Gly-Gly-AMC (calculated mass 8454). This species is formed by trypsin-catalyzed transpeptidation at Arg^{72} instead of at the preferred Arg^{74} and is hydrolyzed by UCH-L3 with the following constants: k_c = 0.03 s^{-1}, K_m = 2 × 10^{-7} M, and k_c/K_m = 1.7 × 10^5 M^{-1} s^{-1}.

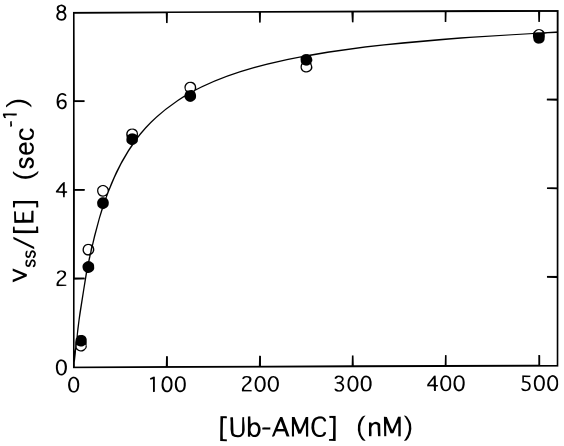

FIGURE 3: Dependence of v_{ss} on substrate concentration for the UCH-L3-catalyzed hydrolysis of Ub-AMC. The reaction was conducted at 25 °C in a pH 7.8 assay buffer containing 50 mM HEPES, 0.5 mM EDTA, 1 mg/mL ovalbumin, and 1 mM DTT. In this experiment, the concentration of UCH-L3 was 10 pM. The data sets from two independent experiments are shown here and were fit to the Michaelis−Menten equation to provide the following nonlinear least-squares parameters: $k_c = 8.08 \pm 0.39$ s^{-1}, $K_m = (3.86 \pm 0.54) \times 10^{-8}$ M, and $k_c/K_m = (2.09 \pm 0.22) \times 10^8$ M^{-1} s^{-1}.

Table 1: Summary of Steady-State Kinetic Parameters for Hydrolysis of Ub-AMC by UCH-L3 and IPaseT[a]

	k_c (s^{-1})	$10^6 \times K_m$ (M)	$10^{-6} \times k_c/K_m$ (M^{-1} s^{-1})
UCH-L3	8.1	0.039	210
IPaseT			
0 μM Ub	0.33	1.4	0.24
0.5 μM Ub	0.68	0.17	4.0

[a] Steady-state velocities were determined at 25 °C in a pH 7.5 assay buffer containing 50 mM HEPES, 0.5 mM EDTA, 0.1 mg/mL ovalbumin, and 1 mM DTT. See text for details of experiments.

experiments are shown in Figure 3 and were fit to the Michaelis−Menten equation to provide the nonlinear least-squares parameters $k_c = 8.08 \pm 0.39$ s^{-1}, $K_m = (38.6 \pm 5.4) \times 10^{-9}$ M, and $k_c/K_m = (209 \pm 22) \times 10^6$ M^{-1} s^{-1} (see Table 1).

Similar values of k_c were determined for Ub-OEt (*28*) and Ub-Lys (*18*) and suggest that deacylation rate limits the process that is governed by k_c (see Discussion below). Interestingly, K_m for Ub-OEt is 0.5 μM and 10-fold higer than the K_m we determined for Ub-AMC (*28*). Since acylation is rapid relative to deacylation, K_m equals $k_3((k_{-1} + k_2)/k_1k_2)$ (see Scheme 1). Thus, since k_3 must be identical for the two substrates and k_1 is likely identical for the two substrates, the 10-fold difference in K_m is due to the ratio k_2/k_{-1} being 10-fold smaller for Ub-OEt than for Ub-AMC. This means that the Michaelis complex formed from interaction of Ub-OEt with UCH-L3 is 10-fold less stable than the Michaelis complex formed from interaction of Ub-AMC with UCH-L3 and may reflect a stabilizing interaction between the enzyme and the hydrophobic AMC moiety of the substrate.

Viscosity-Dependence of Steady-State Kinetic Parameters for the UCH-L3-Catalyzed Hydrolysis of Ub-AMC. k_c/K_m for hydrolysis of Ub-AMC by UCH-L3 is 2×10^8 M^{-1} s^{-1} and approaches the diffusion-controlled limit of 10^9 M^{-1} s^{-1} that is predicted for association of two small proteins. A value for k_c/K_m of similar magnitude was previously reported for the UCH-L3-catalyzed hydrolysis of the Ub-DTT thioester (*18*). To probe for a rate-limiting, diffusion-controlled process, we determined the dependence of steady-state kinetic parameters on viscosity. At various concentrations of two viscogens, glycerol and sucrose, we measured steady-state velocities at eight concentrations of Ub-AMC that ranged from 2 to 250 nM. The resultant data sets were then fit to the Michaelis−Menten equation to yield the parameter estimates of Table 2. These results are plotted as dependencies of k_c and k_c/K_m on relative viscosity in Figure 4. Inspection of these data reveals that the steady-state parameters vary with solvent viscosity and that while these dependencies are complex (see Discussion) they are clearly on viscosity and not on the concentration or chemical identity of the viscogen. Further analysis of these results is given in the Discussion section.

Table 2: Effect of Viscosity on Steady-State Kinetic Parameters for the UCH-L3-Catalyzed Hydrolysis of Ub-AMC[a]

η/η_o (concn)	$10^{-6} \times k_c/K_m$ (M^{-1} s^{-1})	k_c (s^{-1})	$10^9 \times K_m$ (M)
viscogen: glycerol			
1.00	209	8.08	38.6
1.33 (10%, 1.1 M)	273	8.77	32.0
1.84 (20%, 2.2 M)	340	6.65	19.6
2.67 (30%, 3.3 M)	222	3.10	13.9
4.11 (40%, 4.4 M)	82	1.04	12.7
viscogen: sucrose			
1.00	209	8.08	38.6
1.34 (10%, 0.3 M)	294	8.46	28.7
1.96 (20%, 0.6 M)	222	6.48	29.1
3.21 (30%, 0.9 M)	134	2.75	20.5
5.21 (40%, 1.2 M)	60	0.80	13.3

[a] Steady-state kinetic parameters were estimated by nonlinear least-squares fit of the dependence of v_{ss} on Ub-AMC concentration to the simple Michaelis−Menten equation. In all cases, eight substrate concentrations were used that ranged from 2 to 250 nM. Parameter estimates from the least-squares fit have errors less than 10%.

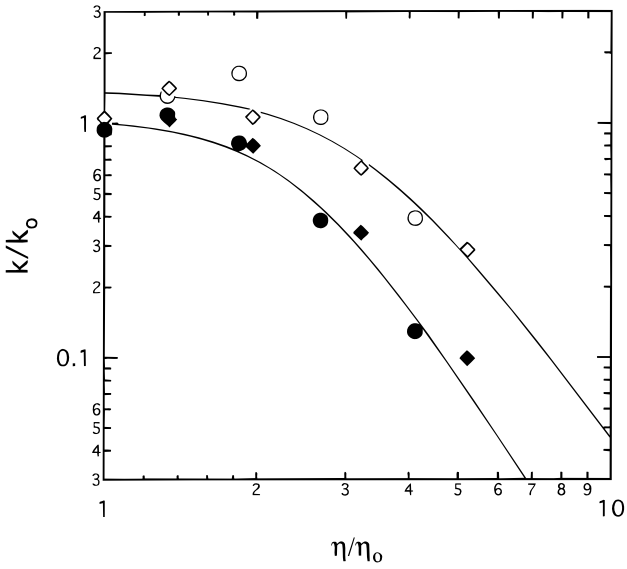

FIGURE 4: Viscosity dependence of steady-state parameters for the UCH-L3-catalyzed hydrolysis of Ub-AMC. Filled symbols are k_c; open symbols are k_c/K_m. Circles are glycerol; diamonds are sucrose. The solid lines through the data for k_c and k_c/K_m were drawn using eqs 10 and 11, respectively, and the following parameters: $k_{-1}/k_2 = 0.02$, $k_3/k_2 = 0.05$, $\delta_1 = \delta_{-1} = 0.2$, and $\delta_2 = 3.2$.

Inhibition of UCH-L3 by Ubiquitin Aldehyde. To determine the dissociation constant for the inhibition of UCH-L3

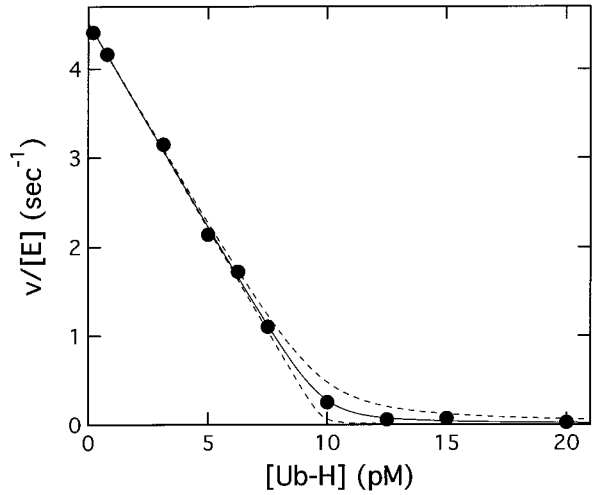

FIGURE 5: Titration of UCH-L3 with Ub-H. In this experiment, various concentrations of Ub-H were incubated with 10 pM UCH-L3 for 4 h at 25 °C in assay buffer. Residual peptidase activity was measured at the end of the incubation and plotted here as $v_{residual}$/[UCH-L3] vs [Ub-H]. The solid line through the data was drawn using eq 1 and the following best-fit parameters: $(v/[E])_o = 4.52 \pm 0.42$ s^{-1}, [UCH-L3] = $(9.76 \pm 0.14) \times 10^{-12}$ M, and $K_i = (47 \pm 17) \times 10^{-15}$ M. The dashed line below the solid was drawn using eq 1 and the following parameters: [UCH-L3] = 10×10^{-12} M and $K_i = 5 \times 10^{-15}$ M. The dashed line above the solid line was drawn using eq 1 and the following parameters: [UCH-L3] = 10×10^{-12} M and $K_i = 150 \times 10^{-15}$ M.

by Ub-H, we conducted enzyme titration experiments in which residual activity is measured for enzyme reaction solutions in which $[I]_o \sim [E]_o > K_i$. Data from such an experiment are plotted in Figure 5 as relative residual activity vs Ub-H concentration. To determine the K_i value, we fit the data to the expression of eq 1 for tight-binding inhibition (*23*, *24*).

$$\frac{v_{is}}{v_c} = \frac{1}{2[E]_o}\{([E]_o - [I]_o - K_i) + \sqrt{([I]_o + K_i - [E]_o)^2 + 4K_i[E]_o}\} \quad (1)$$

This analysis provides the following parameter estimates: $K_i = (47 \pm 17) \times 10^{-15}$ M and [UCH-L3] = $(9.8 \pm 0.1) \times 10^{-12}$ M. The enzyme concentration derived from this exercise is identical to the nominal concentration of UCH-L3 of 10 pM that was used in these experiments.

Although the error estimate that is associated with the calculated K_i value suggests that we know this parameter with ~40% certainty, examination of Figure 5 indicates that the estimate of $K_i = 47 \times 10^{-15}$ M actually rests on the accuracy of the data point at [Ub-H] = 10 pM and that the K_i of 47×10^{-15} M may be an underestimate of the true potency of Ub-H. All things considered, we estimate that $K_i < 50 \times 10^{-15}$ M.

We also sought to determine the kinetics of inhibition of UCH-L3 by Ub-H. Inhibition progress curves for experiments in which UCH-L3 (1 pM) was added to a thermally equilibrated solution of Ub-AMC (10 nM) and several concentrations of Ub-H (25 pM ≤ [Ub-H] ≤ 100 pM) could be fit by a simple exponential rate law at all Ub-H concentrations. These values of k_{obs} are linearly dependent on [Ub-H] with a slope of $(3.5 \pm 0.4) \times 10^7$ M^{-1} s^{-1}. The linearity of this dependence is consistent with a simple, one-step mechanism in which formation of the stable enzyme−inhibitor complex that accumulates in the steady state is governed by the second-order rate constant k_{on} while dissociation of this complex is governed by the first-order rate constant k_{off}. According to this model, the slope of 3.5×10^7 M^{-1} s^{-1} is $k_{on,obs}$ which, for competitive inhibition, equals $k_{on}/(1+ [S]/K_m)$. Thus, given [S] = 10 nM and K_m = 39 nM, we can calculate: $k_{on} = (4.4 \pm 0.5) \times 10^7$ M^{-1} s^{-1}.

This value of k_{on} and a dissociation constant that is less than 50×10^{-15} M allow us to estimate $k_{off} < 2 \times 10^{-6}$ s^{-1}. Clearly, the very small magnitude of this predicted value of k_{off} presents extreme technical problems in its accurate estimation.

In an attempt to measure k_{off}, we conducted an experiment in which a solution of preformed UCH-L3−Ub-H complex was treated with 20 mM semicarbazide. The strategy of this experiment was to trap the free aldehyde as the semicarbacone after it dissociates from UCH-L3−Ub-H. Over the course of 8 days, a small percent of original UCH-L3 could be recovered (data not shown). In control experiments, in which semicarbazide was left out of the reaction mixture, no activity was recovered. These results indicate that inhibitor dissociates from the complex as intact aldehyde that can recombine with enzyme. This is a significant point and is discussed further below. Unfortuately, the results of these experiments were not of sufficient quality to calculate an accurate value for k_{off}, but we can say that $k_{off} < 10^{-8}$ s^{-1}. Thus, from the k_{on} value and this result, we calculate $K_i < 3 \times 10^{-16}$ M.

Kinetics of IPaseT-Catalyzed Hydrolysis of Ub-AMC. Previously we reported that the peptidase activity of IPaseT is modulated by ubiquitin (*9*). Specifically, we found that while submicromolar concentrations of Ub activate IPaseT, higher concentrations are inhibitory. We also found that inhibition of IPaseT by Ub-H is modulated by Ub in the same way with the dissociation constant decreasing with increasing Ub concentration (*17*). Given these results, it was of some interest to see whether Ub has a similar effect on IPaseT during the hydrolysis of Ub-AMC.

To this end, we determined the dependence of v_{ss} on [Ub-AMC] at seven Ub concentrations that ranged from 0 to 5 μM. At each Ub concentration, the dependence of v_{ss} on Ub-AMC concentration (where 4 nM ≤ [Ub-AMC] ≤ 1000 nM) was fit to the Michaelis−Menten equation to provide estimates of steady-state kinetic parameters. Estimated values of k_c/K_m, k_c, and K_m are plotted as a function of Ub concentration in Figure 6.

The biphasic dependence of k_c/K_m on [Ub] can be fit to the two-term, mechanism-independent expression of eq 2 to

$$k_c/K_m = \frac{(k_c/K_m)_1}{1 + \frac{[Ub]}{K_\alpha} + \frac{[Ub]^2}{K_\alpha K_\beta}} + \frac{(k_c/K_m)_2}{\frac{K_\alpha}{[Ub]} + 1 + \frac{[Ub]}{K_\beta}} \quad (2)$$

provide parameter estimates: $(k_c/K_m)_1 = (0.194 \pm 0.019) \times 10^6$ M^{-1} s^{-1}; $(k_c/K_m)_2 = (4.70 \pm 0.27) \times 10^6$ M^{-1} s^{-1}; $K_\alpha = (0.094 \pm 0.020) \times 10^{-6}$ M; $K_\beta = (4.9 \pm 1.3) \times 10^{-6}$ M.

The dependence of k_c on [Ub] is monotonic and can be fit to the simpler expression of eq 3. Parameter estimates are $k_{c,1} = 0.339 \pm 0.050$ s^{-1}, $k_{c,2} = 0.723 \pm 0.015$ s^{-1}, and $K_\gamma = (0.31 \pm 0.12) \times 10^{-6}$ M. In the next section, we will

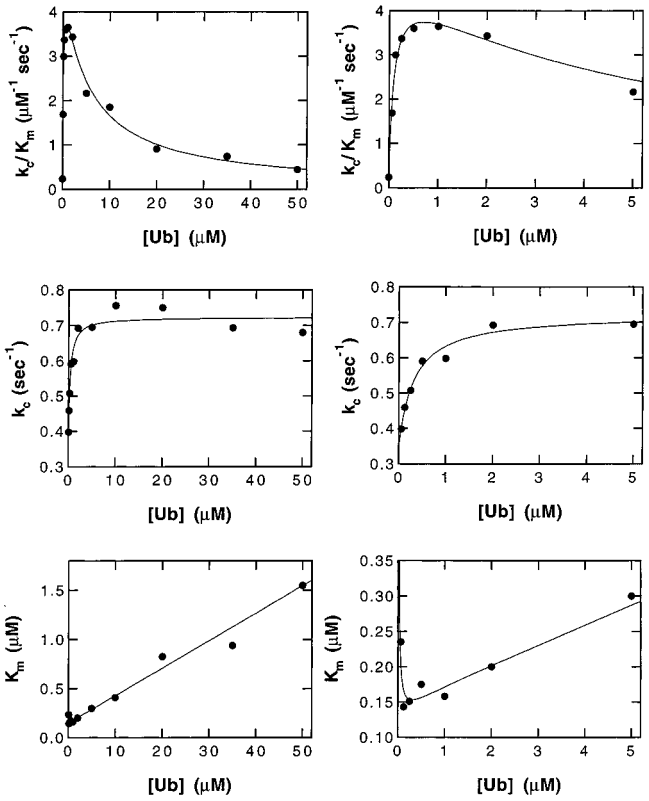

FIGURE 6: Ub concentration dependence of steady-state parameters for the IPaseT-catalyzed hydrolysis of Ub-AMC. Steady-state kinetic parameters for the hydrolysis of Ub-AMC by UCH-L3 were determined at various concentrations of Ub from the dependence of steady-state velocity on Ub-AMC. Michaelis−Menten plots of v_{ss} vs [Ub-AMC] (data not shown) were well behaved and provided values of k_c, K_m, and k_c/K_m with errors of 10% or less (parameter estimation by nonlinear least-squares fit of data). Reactions were conducted at a final 25.0 ± 0.02 °C in an assay buffer of 20 mM HEPES, 0.5 mM EDTA, pH 7.8, containing 1 mg/mL ovalbumin and 10 mM DTT and with a final IPaseT concentration of 2 nM.

$$k_c = \frac{k_{c1}}{1 + \dfrac{[Ub]}{K_\gamma}} + \frac{k_{c2}}{\dfrac{K_\gamma}{[Ub]} + 1} \tag{3}$$

analyze these data in the context a Ub-dependent mechanism for IPaseT.

DISCUSSION

In this paper, we report the preparation of Ub-AMC and its utility as a substrate for UCH-L3 and IPaseT. From our studies, three areas emerge as topics for discussion: Viscosity-Dependent UCH-L3 Catalysis, Inhibition of UCH-L3 by Ub-H, and Ubiquitin-Dependent IPaseT Catalysis. We end the Discussion with general considerations about catalysis by deubiquitinating enzymes.

Viscosity-Dependent Catalysis by UCH-L3. Hydrolysis of Ub-AMC by UCH-L3 proceeds with a k_c/K_m value of 2×10^8 M^{-1} s^{-1}, a value that is similar to estimates of second-order rate constants for diffusion-controlled association of two proteins of this size. To investigate the possibility that reaction of Ub-AMC with UCH-L3 may be rate-limited by diffusion, we examined the viscosity dependence of k_c/K_m for this reaction. In the course of these studies, we also collected data on the viscosity dependence of k_c. As evident in Figure 4, the viscosity dependencies of both kinetic parameters are complex. Both k_c and k_c/K_m display biphasic dependencies on viscosity with insensitivity to viscosity at η/η_o values less than ~2. Higher viscosities result in reductions in reaction rate.

Now, solvent viscosity can influence rates of enzyme-catalyzed reactions by two principle mechanisms: (1) Since molecular diffusion coefficients vary inversely with the viscosity of the medium, an increase in solvent viscosity will lead to a decrease in the association rate of an enzyme and substrate. This will manifest itself in a viscosity-dependent decrease in k_c/K_m for reactions in which the process that is governed by k_c/K_m is diffusion-controlled. (2) Since solvent viscosity dampens structural fluctuations of proteins through frictional effects, increases in solvent viscosity will lead to decreases in reaction rates for catalytic processes that are dependent on enzyme structural fluctuations (*25, 26*). This will manifest itself in a viscosity-dependent decrease in k_c for reactions in which fluctuations of the enzyme are part of the reaction coordinate for the process that is governed by k_c. Both of these mechanisms give rise to the same general kinetic expression:

$$k = \frac{k_B T}{h} \eta^{-\delta} \exp\left(\frac{-\Delta G^{\ddagger}}{RT}\right) \tag{4}$$

where η is solvent viscosity and δ is a coupling constant that measures the sensitivity of a reaction to solvent viscosity.

In typical analyses of viscosity-dependent reactions, one expresses the relative reaction velocity as a function of relative viscosity. This leads to the expressions

$$k/k_o = (\eta/\eta_o)^{-\delta} \tag{5}$$

$$\log(k/k_o) = -\delta \log(\eta/\eta_o) \tag{6}$$

where k_o and η_o are the rate constant and viscosity, respectively, in aqueous buffer containing no added viscogen. Theory predicts that δ can vary from 0 to 1 (*25*−*27*). δ will be near 0 for reactions of enzymes whose active sites are largely uncoupled to solvent. On the other hand, δ will be near 1 for reactions of enzymes whose active sites are tightly coupled to solvent. Coupling of active sites and catalytic processes to solvent is thought to occur through dynamic fluctuations of the enzyme protein.

The dependencies of k_c/K_m and k_c on viscosity (Figure 4) clearly indicate complex kinetic situations that cannot be accounted for with the simple expression of eq 6. However, both dependencies can be fit by variants of the general expression of eq 7, which expresses the viscosity dependence

$$\frac{k}{k_o} = \left(\frac{\eta}{\eta_o}\right)^{-\delta} \left\{\frac{1+\alpha}{\left(\dfrac{\eta}{\eta_o}\right)^{-\delta} + \alpha}\right\} \tag{7}$$

of a rate constant, k, for a two-step reaction where one step is viscosity-dependent (k_1) and the other reaction step (k_2) is viscosity-independent. α is the ratio of the rate constants for the two steps (i.e., k_2/k_1) at $\eta/\eta_o = 1$.

Also, since both k_c and k_c/K_m display similar, biphasic viscosity dependencies, it is a reasonable assumption that the processes that are governed by these two parameters share a common viscosity-dependent step. We can identify this step if we examine the likely kinetic mechanism for UCH-

L3 (Scheme 1) and the rate expressions for k_c and k_c/K_m that are derived from this mechanism:

$$k_c = \frac{k_2 k_3}{k_2 + k_3} \tag{8}$$

$$\frac{k_c}{K_m} = \frac{k_1 k_2}{k_{-1} + k_2} \tag{9}$$

We can account for the data of Figure 4 if we assume that k_1, k_{-1}, and k_2 are viscosity-sensitive and that k_3 is viscosity-insensitive. Given these conditions, the following expressions can be derived:

$$\frac{k_c}{k_{co}} = \left(\frac{\eta}{\eta_o}\right)^{-\delta 2}\left\{\frac{1 + \frac{k_{3o}}{k_{2o}}}{\left(\frac{\eta}{\eta_o}\right)^{-\delta 2} + \frac{k_{3o}}{k_{2o}}}\right\} \tag{10}$$

$$\frac{k_c/K_m}{(k_c/K_m)_o} = \left(\frac{\eta}{\eta_o}\right)^{-(\delta 1 + \delta 2)}\left\{\frac{1 + \frac{k_{-1o}}{k_{2o}}}{\left(\frac{\eta}{\eta_o}\right)^{-\delta(-1)}\left(\frac{k_{-1o}}{k_{2o}}\right) + \left(\frac{\eta}{\eta_o}\right)^{-\delta 2}}\right\} \tag{11}$$

The solid lines of Figure 4 were drawn with eqs 10 and 11 and the following parameter estimates: $k_{-1}/k_2 = 0.02$, $k_3/k_2 = 0.05$, $\delta_1 = \delta_{-1} = 0.2$, $\delta_2 = 3.2$, and $\delta_3 = 0$.

The values for k_{-1}/k_2 and k_3/k_2 indicate that acylation of UCH-L3 by Ub-AMC is a relatively rapid process. Given a value of 0.02 for k_{-1}/k_2, k_c/K_m becomes approximately equal to k_1, which is consistent with the very large value of k_c/K_m. Likewise, given a value of 0.05 for k_3/k_2, k_c becomes approximately equal to k_3. Rate-limiting deacylation for k_c is consistent with the reported k_c value of 13 s^{-1} for the UCH-L3-catalyzed hydrolysis of the ester substrate, Ub-OEt (*28*), which is essentially identical to the value of k_c that we report here for the UCH-L3-catalyzed hydrolysis of the amide, Ub-AMC. For both reactions, we propose that k_c is rate-limited by deacylation (i.e., k_3). There is ample evidence for rate-limiting deacylation during protease-catalyzed hydrolysis of specific amides (*29*−*31*).

The relative insensitivity of k_1 to solvent viscosity (i.e., $\delta_1 = 0.2$) suggests that binding of Ub-AMC to UCH-L3 is only partially diffusion-controlled. If k_1 were entirely diffusion-controlled, δ_1 would equal 1.

The value for δ_2 is 3.2 and cannot be easily explained by current theory, which states that values of δ must lie between 0 and 1. However, such a large value is not without precedent. For example, δ values of 1.9 and 2.4 were observed for hydrolysis of the acyl-enzyme formed from reaction of subtilisin BPN′ with Suc-Ala-Ala-Pro-Phe-SBzl (*32*) and for cytochrome *c*-catalyzed electron transfer (*33*), respectively. Neither study provided mechanisms to explain the large values. In the current case, the large value of δ may be explained by a consideration of solvent/protein frictional effects on enzymatic reaction rates (*34*).

The theoretical underpinnings for the effect of solvent viscosity on unimolecular rate processes in the condensed phase is provided by the Kramers theory (*35*), which shows that for diffusive barrier crossings, rates are inversely proportional to friction. To apply the Kramers theory to enzymatic reactions, we must consider two sources of friction that can affect protein fluctuations (*34*): the friction of the solvent, which retards the motion of atoms on the surface of the protein, and the internal friction of the protein, which slows the motion of protein atoms relative to each other. In the current situation, involving reaction within a Michaelis complex comprising two proteins, the combined external and internal frictional effects may manifest themselves in a δ value that is larger than unity. Additional studies of the viscosity dependence of protein−protein interactions may help to illuminate this point.

Inhibition of UCH-L3 by Ub-H. In this study, we demonstrate that Ub-H is an exceptionally potent inhibitor of UCH-L3 with an estimated K_i value that lies between 10^{-16} and 10^{-14} M. However, even this range underestimates the true potency of Ub-H if inhibition involves formation of a hemithioacetal at the active site of UCH-L3 since the predominant form of Ub-H in aqueous buffer is the hydrate. To accurately reflect the binding affinity, the observed dissociation constant must be corrected for the hydration of Ub-H (*36*, *37*). This correction is according to

$$K_{i,corr} = \frac{K_i}{1 + K_{hyd}[H_2O]} \tag{12}$$

where

$$K_{hyd}[H_2O] = [\text{hydrate}]/[\text{aldehyde}] \tag{13}$$

Since $K_{hyd}[H_2O]$ is ∼10 for aldehydes of general structure $RNHCH_2C(O)H$ (*36*, *37*), we can calculate that $10^{-17} < K_{i,corr} < 10^{-15}$ M. This range reflects the true affinity of UCH-L3 for Ub-H.

The observed association rate constant must also be corrected for hydration of the aldehyde. Thus, $k_{on,corr} = 10k_{on} = 10(4.4 \times 10^7\ M^{-1}\ s^{-1}) = 4.4 \times 10^8\ M^{-1}\ s^{-1}$. This value is identical to k_c/K_m for the reaction of UCH-L3 with Ub-AMC and suggests that association of UCH-L3 with Ub-H is partially diffusion-controlled, like the reaction of UCH-L3 with Ub-AMC.

We can explain the extreme potency of Ub-H in terms of the energetics of transition-state analogue inhibition (*38*). For an enzyme-catalyzed reaction, the enzyme will bind a "perfect" transition state analogue inhibitor with the same affinity that it binds the transition state for the reaction it is catalyzing (*38*). Less than ideal inhibitors will of course be bound by the enzyme less tightly.

The free-energy correlation of Figure 7 supports the notion that Ub-H is a transition state analogue inhibitor of deubiquitinating enzymes. In this figure, we plot $-\Delta G_{ass}$ for the inhibition of deubiquitinating enzymes by Ub-H or Z-Leu-Arg-Gly-Gly-H as a function of $-\Delta G^{\ddagger}$ calculated from k_c/K_m for deubiquitinating enzyme-catalyzed hydrolysis of the corresponding AMC substrates. Since several ΔG values were calculated from poorly defined rate or dissociation constants (see Table 3), this analysis must be regarded as only semiquantitative. However, even with this cavaet, the correlation is linear with a slope near unity. This indicates that each free-energy increment of transition-state stabilization can be translated into binding energy for stabization of the E−I complex. Thus, the stable complex formed from

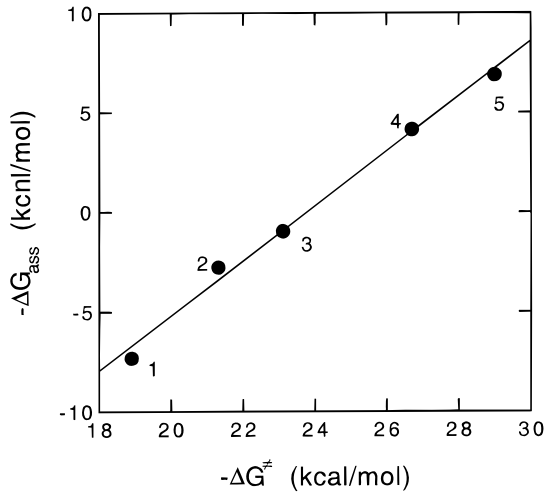

FIGURE 7: Linear free-energy correlation for deubiquitinating enzyme catalysis and inhibition. Values of $-\Delta G_{ass}$ and $-\Delta G^{\ddagger}$ from Table 3 are correlated in this figure. 1, UCH-L3 + Ub-X; 2, IPaseT ([Ub] = 0.5 μM) + Ub-X; 3, IPaseT ([Ub] = 0 μM) + Ub-X; 4, IPaseT ([Ub] = 0.5 μM) + Z-Leu-Arg-Gly-Gly-X; and 5, UCH-L3 + Z-Leu-Arg-Gly-Gly-X. X = AMC or H. The best fit has a slope of 1.38 ± 0.06.

Table 3: Correlation of Deubiquitinating Enzyme Catalysis and Inhibition

system[a]	k_c/K_m (M^{-1} s^{-1})	$K_{i,corr}^{-1}$ (M^{-1})	$-\Delta G^{\ddagger b}$ (kcal/mol)	$-\Delta G_{asn}{}^{c}$ (kcal/mol)
UCH-L3 Ub-X	2×10^8	$>2 \times 10^{14}$	18.9	−7.32
IPaseT ([Ub] = 0.5 μM) Ub-X	4×10^6	$>1 \times 10^{11}$	21.3	−2.76
IPaseT ([Ub] = 0 μM) Ub-X	2×10^5	5×10^9	23.1	−0.97
IPaseT ([Ub] = 0.5 μM) Z-Leu-Arg-Gly-Gly-X	5×10^2	8×10^5	26.7	4.14
UCH-L3 Z-Leu-Arg-Gly-Gly-X	<10	$>1 \times 10^4$	29.0	6.90

[a] X = AMC or H. [b] $-\Delta G^{\ddagger}$, the activation free energy, was calculated according to the following equation: $-\Delta G^{\ddagger} = RT \ln((k_c/K_m[E]_{stdstate})/(k_B T/h))$, where $[E]_{stdstate} = 10^{-9}$ M and $T = 298$ °C. [c] $-\Delta G_{ass}$, the free energy of association, was calculated according to the following equation: $-\Delta G_{ass} = RT \ln([I]_{stdstate}/K_{icorr})$, where $[I]_{stdstate} = 10^{-9}$ M and $T = 298$ °C.

interaction of UCH-L3 with Ub-H has structural analogy to catalytic transition states for reactions of UCH-L3.

If we accept that Ub-H is a transition-state analogue inhibitor of deubiquitinating enzymes, theory allows us to calculate the limiting K_i value for the "perfect" transition-state analogue inhibitor (*38*). This limiting value is equal to $K_{\neq}$, the dissociation constant for binding of the transition state for the uncatalyzed reaction to the enzyme. $K_{\neq}$ can be calculated from eq 14, which is based on the thermodyamic

$$k_c/K_s = k_u/K_{\neq} \qquad (14)$$

cycle of Scheme 2. In this equation, k_u is the first-order rate constant for the uncatalyzed reaction. For the inhibition of UCH-L3 by Ub-H, we can calculate a value of 1.5×10^{-17} M for $K_{\neq}$ using $k_c/K_m = 2 \times 10^8$ M^{-1} s^{-1} for the UCH-L3-catalyzed hydrolysis of Ub-AMC and $k_u = 3 \times 10^{-9}$ s^{-1} (*39*). This value falls within the range of the estimated value for $K_{i,corr}$ for inhibition of UCH-L3 by Ub-H and indicates that the structure of the hemithioacetal formed from interaction of UCH-L3 with Ub-H closely resembles the catalytic transition state for UCH-L3-catalyzed hydrolyses and that Ub-H is a "perfect" transition-state analogue inhibitor.

Scheme 2: Transition-State Binding Energy in Enzymatic Catalysis

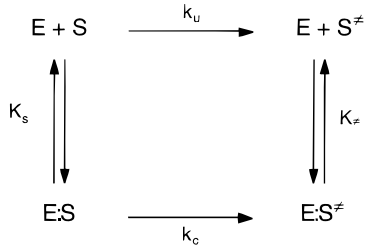

Given the extraordinary potency of Ub-H, we must comment further on, and possibly question, the assumption that is implicit in the above analysis: The stable complex that is formed from interaction of UCH-L3 and Ub-H is a hemithioacetal that collapses back to liberate chemically unmodified UCH-L3 and Ub-H. And the corollary to this assumption is the following: the binding energy that stabilizes the hemithioacetal formed from interaction of UCH-L3 with Ub-H is the same binding energy that stabilizes catalytic transition states during UCH-L3-catalyzed hydrolyses of C-terminal derivitives of Ub.

Now, support for this assumption can be found in the results of our experiments in which we find that reversal of inhibition can only be observed when the released Ub-H is trapped as its semicarbazone. This is supported by previous results of Rose and Pickart (*19*), who found that acid denaturation of the complex of UCH-L3 and Ub-H releases the aldehyde quantitatively. Furthermore, there is ample evidence given in the literature that a hemithioacetal forms during interaction of thiol proteases with peptide aldehydes (*40, 41*). Under ordinary circumstances, together these results would argue strongly in support of our assumption. However, the extraordinarily small value of k_{off} clearly raises a red flag. We are forced to entertain the possibility that, once formed, the hemithioacetal undergoes UCH-L3-catalyzed transformation to another species that is stabilized through covalent chemical interactions with active site enzyme residues and not through transition-state-stabilizing interactions. If such a mechanism obtains, the small magnitude of k_{off} is due to slow, chemical decomposition of stable but reversibly formed covalent bonds. This contrasts with our presumed mechanism of transition-state analogue inhibition in which the small magnitude of k_{off} is due to the stability of the transition-state-like hemithioacetal. The stability of this species derives from active site chemistry that is energetically coupled to remote, noncovalent protein−protein interactions.

These two mechanistic alternatives for inhibition of UBC_{30K} by Ub-H are illustrated in the free-energy diagrams of Scheme 3. In both cases, interaction of enzyme and inhibitor is partially rate-limited by both association to form the encounter complex E-SH−Ub-H and subsequent attack of the thiol on the aldehydic carbon to form the hemithioacetal. This draws on analogy to the rate-limiting steps for k_c/K_m for UCH-L3-catalyzed hydrolysis of Ub-AMC (see above). For the mechanism involving transition-state inhibition, the hemithioacetal is the species that accumulates and

Scheme 3: Free-Energy Diagrams for Inhibition of UBC_{30K} by Ub-H[a]

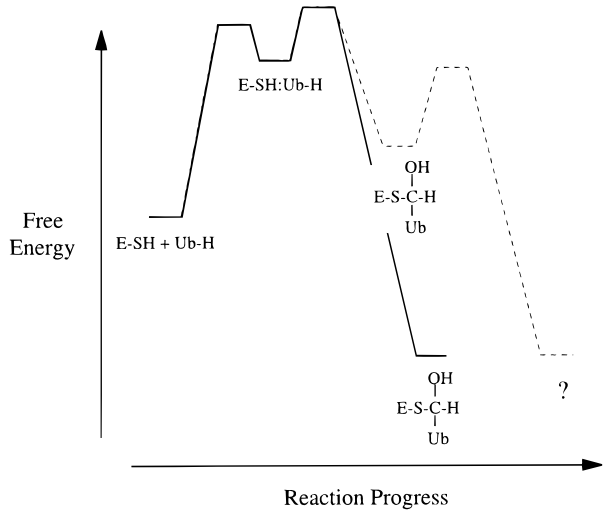

[a] The solid line represents a mechanism for transition-state analogue inhibition involving stabilization of a hemithioacetal intermediate, and the dashed line represents a mechanism of inhibition in which the hemithioacetal that forms is transformed to the final stable species. See text for details.

k_{off} is slow due to the great stability of the hemithioacetal. For the other mechanistic alternative, an unknown chemistry converts the hemithioacetal to the stable species and k_{off} is slow due to the great stability of this species.

In either case, the mechanistic explanation for the small magnitude of k_{off} is unprecedented and represents a radical mechanistic departure from all other interactions between thiol proteases and even their most specific peptide aldehyde inhibitors. Determining which mechanism is at work is currently underway.

Ubiquitin-Dependent Catalysis by IPaseT. One of the best studied members of the UBP gene family is isopeptidase T (*4*, *6*, *7*, *9*, *16*). This enzyme is thought to trim Ub monomers from the C-termini of polyUb chains (*4*, *6*, *7*) and, thus, may play a role in the regulation of protein turnover through the ubiquitin−proteasome pathway by preventing the buildup of free polyUb chains which are known to inhibit the 26S proteasome complex (*6*). Previously, we reported a series of low-molecular-weight peptide-AMC substrates for IPaseT (e.g., Z-Leu-Arg-Gly-Gly-AMC) that are based on the C-terminus of Ub (*8*). In the course of these studies, we discovered that Ub modulates the kinetics of these reactions. Specifically, we found that while submicromolar concentrations of Ub activate IPaseT, higher concentrations are inhibitory (Table 4). In the activation phase, k_c/K_m for the IPaseT-catalyzed hydrolysis of Z-Leu-Arg-Gly-Gly-AMC increases 50-fold relative to k_c/K_m for unactivated IPaseT. This activation occurs with a K_d for Ub of 0.1 μM. At higher concentrations, Ub is inhibitory and titrates k_c/K_m with a K_i of 3 μM. An interesting feature of this inhibition is that it is only partial; that is, even at very high concentrations of Ub, the velocity does not go to zero. This suggests that the complex present under these conditions, namely, Ub−E−S−Ub, is catalytically competent. We also found that the dissociation constant for inhibition of IPaseT by Ub-H is modulated by Ub in the same way (see Table 4). Given these results, it was of some interest to see whether Ub has a similar effect on IPaseT during the hydrolysis of Ub-AMC.

Table 4: Comparison of Steady-State Kinetic Parameters for Catalysis by IPaseT

	Z-LRGG-AMC	Ub-AMC	Ub-H
k_c (s^{-1})			
[Ub] = 0 μM	0.05	0.33	
[Ub] = 0.5 μM	0.09	0.68	
ratio	2	2	
k_c/K_m (M^{-1} s^{-1})			
[Ub] = 0 μM	30	240000	
[Ub] = 0.5 μM	510	4000000	
ratio	17	16	
$10^9 \times K_i$ (M)			
[Ub] = 0 μM			2.3
[Ub] = 0.5 μM			<0.1
ratio			23

Scheme 4: Minimal Kinetic Mechanism for IPaseT-Catalyzed Hydrolysis of Ub-AMC

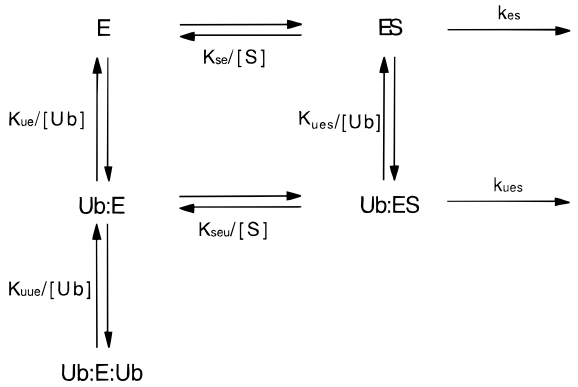

To this end, we determined steady-state kinetic parameters for the IPaseT-catalyzed hydrolysis of Ub-AMC as a function of Ub concentration. These data are shown in Figure 6 and can be fit to the mechanism-independent expressions of eqs 2 and 3. Inspection of the data in Figure 6 reveals that the dependence of k_c/K_m on Ub concentration is similar to the Ub dependence that we reported previously for the IPaseT-catalyzed hydrolysis of peptide substrates: Ub activates at low concentration and inhibits at high concentration. Furthermore, the ubiquitin dissociation constants, K_α and K_β, that we determined with Ub-AMC are identical to those values determined previously in two independent studies (*9*, *17*).

The simplest kinetic mechanism that can account for these data is shown in Scheme 4.[3] This mechanism differs from the kinetic mechanism for hydrolysis of Z-Leu-Arg-Gly-Gly-AMC (see Scheme 1 of ref *9*) in that Ub-AMC cannot combine with Ub−E−Ub to form the catalytically competent species Ub−ES−Ub. Thus, unlike the IPaseT-catalyzed hydrolysis of Z-Leu-Arg-Gly-Gly-AMC where only partial inhibition by Ub is observed, the hydrolysis of Ub-AMC can be completely inhibited by Ub as demonstrated in Figure 6, where we see that high concentrations of Ub drive k_c/K_m

[3] In this paper, rate constant nomenclature for IPaseT follows the conventions of our previous paper (*9*) and is according to the following rules: (1) First-order catalytic constants have subscripts that correspond to the complex that is turning over. Thus, k_{es} is the first-order rate constant for the turnover of the Michaelis complex E−S. (2) Dissociation constants have subscripts that correspond to the complex that is dissociating; the first letter of the subscript refers to the substance that is dissociating from the enzyme complex. Thus, K_{seu} is the dissociation constant for the breakdown of Ub−ES to S and Ub−E.

to zero. The kinetic difference between inhibition of IPaseT-catalyzed hydrolysis of these two substrates can be explained by steric hindrance: Unlike Z-Leu-Arg-Gly-Gly-AMC, Ub-AMC is too large to bind to Ub−E−Ub.

This kinetic mechanism of Scheme 4 also predicts a simple dependence of k_c on [Ub], with k_{es} increasing monotonically to k_{ues}. This prediction is borne out by experiment (Figure 6).

A more detailed, quantitative analysis of the results of Figure 6 and Scheme 4 begins with consideration of the rate equation that describes the mechanism of Scheme 4:

$$\frac{v_{ss}}{[E]_o} = \frac{\dfrac{k_{es}[S]}{K_{se}+[S]}}{1+\dfrac{[Ub]}{K_{ue}'}+\dfrac{[Ub]^2}{K_{ue}'K_{uue}'}} + \frac{\dfrac{k_{ues}[S]}{K_{seu}+[S]}}{\dfrac{K_{ue}'}{[Ub]}+1+\dfrac{[Ub]}{K_{uue}'}} \quad (15)$$

In this equation,

$$K_{ue}' = K_{ue}\frac{1+[S]/K_{se}}{1+[S]/K_{seu}} \quad (16)$$

and

$$K_{uue}' = K_{uue}(1+[S]/K_{seu}) \quad (17)$$

From these expressions, the following can be derived:

$$k_c/K_m = \frac{k_{es}/K_{se}}{1+\dfrac{[Ub]}{K_{ue}}+\dfrac{[Ub]^2}{K_{ue}K_{uue}}} + \frac{k_{ues}/K_{seu}}{\dfrac{K_{ue}}{[Ub]}+1+\dfrac{[Ub]}{K_{uue}}} \quad (18)$$

$$k_c = \frac{k_{es}}{1+\dfrac{[Ub]}{K_{ue}(K_{seu}/K_{se})}} + \frac{k_{ues}}{\dfrac{K_{ue}(K_{seu}/K_{se})}{[Ub]}+1} \quad (19)$$

or

$$k_c = \frac{k_{es}}{1+[Ub]/K_{ues}} + \frac{k_{ues}}{K_{ues}/[Ub]+1} \quad (20)$$

The relationship between the rate parameters in these equations and the rate parameters of eqs 2 and 3 for the mechanism-independent analysis is clear.

A problem emerges upon closer examination of Scheme 4. The mechanism of Scheme 4 predicts that the following equality must hold:

$$K_{se}/K_{seu} = K_{ue}/K_{ues} \quad (21)$$

Three of these equilibrium constants can be estimated from results of our experiments:

$$K_{se} = \frac{k_{es}}{k_{es}/K_{se}} = \frac{0.34\ s^{-1}}{0.19\ \mu M^{-1}\ s^{-1}} = 1.7\ \mu M$$

$$K_{seu} = \frac{k_{ues}}{k_{ues}/K_{seu}} = \frac{0.72\ s^{-1}}{4.7\ \mu M^{-1}\ s^{-1}} = 0.15\ \mu M$$

$$K_{ue} = K_\alpha = 0.094\ \mu M$$

These three values and eq 21 allow us to calculate a value for K_{ues}, the fourth equilibrium constant of the thermodynamic cycle of Scheme 4:

$$K_{ues} = K_{ue}K_{seu}/K_{se} = 0.008\ \mu M$$

This value follows intuitively from the simple thermodynamic rationale that since S is bound 10-fold tighter by Ub−E than by E (i.e., $K_{seu} < K_{se}$), then Ub must be bound 10-fold tighter by ES than by E (i.e., $K_{use} < K_{ue}$). However, this analysis breaks down when we consider the value of K_{ues} that was estimated directly from the dependence of k_c on [Ub] using eq 3 or 20. This value, K_γ, is 0.3 μM and is much larger than the value of 0.008 μM that we just calculated using a thermodynamic analysis of Scheme 4.

Clearly, our results cannot be explained by Scheme 4 and demand a more complex mechanism. Scheme 5 shows an expanded version of the mechanism for Ub-AMC hydrolysis that now includes formation and decomposition of the acyl-enzyme intermediate that must form during the course of deubiquitinating enzyme-catalyzed reactions. Recall that the mechanism of Scheme 4 was originally formulated to explain the IPaseT-catalyzed hydrolysis of peptide substrates such as Z-Leu-Arg-Gly-Gly-AMC, where acylation is rate-limiting and k_c equals k_{es} at low Ub concentrations and k_{ues} at high Ub concentrations. For hydrolysis of Z-Leu-Arg-Gly-Gly-AMC, we have shown that the thermodynamic argument presented above obtains (*9*). However, for the hydrolysis of the more specific substrate Ub-AMC, we must consider two possibilities: (i) k_c may be rate-limited by deacylation, even though the substrate is an amide (*29*−*31*), and (ii) the identity of the rate-limiting step (i.e., acylation or deacylation) may be dependent on Ub concentration. The complexity of this kinetic situation is shown in the rate expression of eq 22.

$$k_c = \left(\frac{k_{es}}{1+\dfrac{[Ub]}{K_{ues}}}+\frac{k_{ues}}{1+\dfrac{K_{ues}}{[Ub]}}\right)\left(\frac{k_{e\text{-}acyl}}{1+\dfrac{[Ub]}{K_{ue\text{-}acyl}}}+\frac{k_{ue\text{-}acyl}}{1+\dfrac{K_{ue\text{-}acyl}}{[Ub]}}\right)\Bigg/ \left[\left(\frac{k_{es}}{1+\dfrac{[Ub]}{K_{ues}}}+\frac{k_{ues}}{1+\dfrac{K_{ues}}{[Ub]}}\right)+\left(\frac{k_{e\text{-}acyl}}{1+\dfrac{[Ub]}{K_{ue\text{-}acyl}}}+\frac{k_{ue\text{-}acyl}}{1+\dfrac{K_{ue\text{-}acyl}}{[Ub]}}\right)\right] \quad (22)$$

At low [Ub], this equation simplifies to

$$k_c = \frac{k_{es}k_{e\text{-}acyl}}{k_{es}+k_{e\text{-}acyl}} \quad (23)$$

While at high [Ub], eq 11 becomes

$$k_c = \frac{k_{ues}k_{ue\text{-}acyl}}{k_{ues}+k_{ue\text{-}acyl}} \quad (24)$$

We can see that at low [Ub], the rate limitation of k_c is dependent on the relative magnitudes of k_{es} and k_{e-acyl}, while at high [Ub], the rate limitation of k_c is dependent on the relative magnitudes of two different rate constants k_{ues} and $k_{ue-acyl}$.

Scheme 5: Mechanism for the IPaseT-Catalyzed Hydrolysis of Ub-AMC

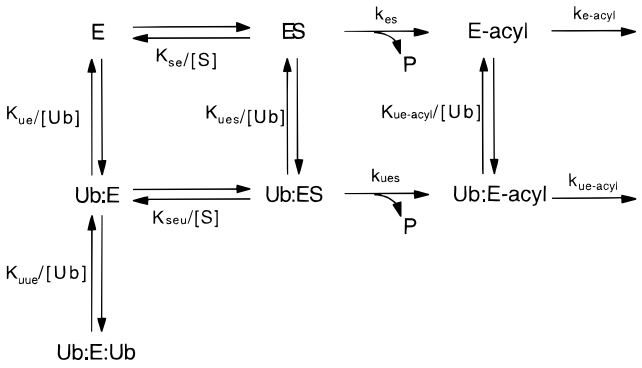

Scheme 6: Energetics of Catalysis by Ubiquitin C-Terminal Hydrolases

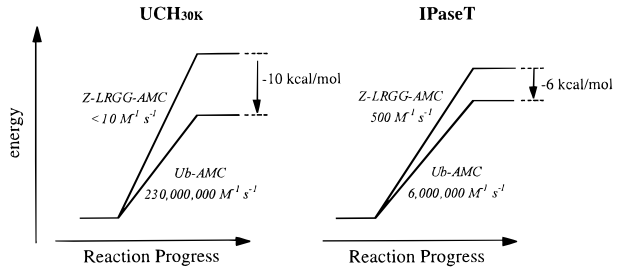

We see that the kinetics of IPaseT-catalyzed hydrolysis of Z-Leu-Arg-Gly-Gly-AMC and Ub-AMC are distinct and lead to quite different thermodynamic outcomes. During hydrolysis of Z-Leu-Arg-Gly-Gly-AMC, the binding of Ub to free enzyme is thermodynamically coupled to the binding of Ub to the Michaelis complex, ES, which is the form of enzyme that accumulates in the steady state during the hydrolysis of this substrate and thus serves as the reactant state for k_c. In contrast, during the hydrolysis of Ub-AMC by IPaseT, if deacylation is rate-limiting, the reactant state for k_c is now the acyl-enzyme, the form of the enzyme that accumulates in the steady state for hydrolysis of Ub-AMC. In this case, binding of Ub to free enzyme is *uncoupled* to the binding of Ub to the acyl-enzyme. This is so because formation of the acyl-enzyme is an irreversible process and therefore hydrolysis of the acyl-enzyme is thermodynamically unlinked to substrate binding and enzyme acylation.

Origins of Catalytic Power for Deubiquitinating Enzymes. A striking feature of catalysis by deubiquitinating enzymes is the very large rate enhancements observed when the substrate is elaborated from the tetrapeptide, Z-Leu-Arg-Gly-Gly-AMC, to Ub-AMC (Table 4). For IPaseT, the ratio of rate constants for hydrolyzes of these substrates is 10^4 ($-\Delta\Delta G^{\ddagger} = 6$ kcal/mol), while for UCH-L3 this ratio is $>10^7$ ($-\Delta\Delta G^{\ddagger} > 10$ kcal/mol). These results speak to two important features of catalysis by deubiquitinating enzymes.

First, deubiquitinating enzymes, as a class, are able to utilize the free energy that is released from remote interactions with Ub-containing substrates for stabilization of catalytic transition states (Scheme 6). Utilization of binding energy for transtition-state stabilization is a principle mechanism by which enzymes catalyze reactions (*42*, *43*) and is common among proteases (*31*, *44*). In the case of deubiquitinating enzymes, 6−10 kcal/mol can be obtained from remote protein−protein interactions between enzyme and Ub-X substrates. This thermodynamic result can be interpreted in a structural context. The crystal structure of UCH-L3 has recently been solved (*45*) and suggests a mechanism for hydolysis of Ub-X substrates in which binding of the ubiquitin portion of the substrate triggers a conformation change of the enzyme which allows the C-terminal tail to bind in the acitve site and undergo $Gly^{76}-X$ bond hydrolysis. We see then that the $-\Delta\Delta G^{\ddagger}$ of 10 kcal/mol for UCH-L3-catalyzed hydrolyzes of Z-Leu-Arg-Gly-Gly-AMC and Ub-AMC reflects the free energy that is liberated when the protein portion of Ub-AMC binds to UCH-L3 and is then used, at least in part, to drive the conformational change that presumably sets up the active site for catalysis.

Second, the smaller UCHs have apparently evolved to more efficiently utilize the energy from these interactions. This must have occurred, at least in part, to compensate for not possessing a binding domain for a Ub "leaving group" (Scheme 6). This would explain why UCH-L3 is able to derive an additional 4 kcal/mol of transition-state binding energy from interaction with Ub-AMC. UBPs, such as IPaseT, are able to make up this energy by interacting with a more extended area of a polyUb chain (*7*, *9*).

ACKNOWLEDGMENT

I thank Dr. Eric Lightcap for his careful reading of the manuscript and helpful comments on the mechanism of slow-binding inhibition of UCH-L3 by Ub-H.

REFERENCES

1. Finley, D., and Chau, V. (1991) *Annu. Rev. Cell. Biol. 7*, 25−69.
2. Ciechanover, A. (1994) *Cell 79*, 13-21.
3. Hochstrasser, M. (1995) *Curr. Opin. Biol. 7*, 215−223.
4. Wilkinson, K. D. (1995) *Annu. Rev. Nutr. 15*, 161−189.
5. Goldberg, A. L., and Mitch, W. (1997) *N. Eng. J. Med. 335*, 1897−1905.
6. Hadari, T., Warms, J. V. B., Rose, I. A., and Hershko, A. (1992) *J. Biol. Chem. 267*, 719−727.
7. Wilkinson, K. D., Tashayev, V. L., O'Conner, L. B., Larsen, C. N., Kasperek, E., and Pickart, C. M. (1995) *Biochemistry 34*, 14535−14546.
8. Mayer, A. N., and Wilkinson, K. D. (1989) *Biochemistry 28*, 166−172.
9. Stein, R. L., Chen., Z., and Melandri, F. (1995) *Biochemistry 34*, 12616−12623.
10. Gray, D. A., Inazawa, J., Gupta, K., Wong, A., Ueda, R., and Takahashi, T. (1995) *Oncogene 11*, 217902183.
11. Papa, F. R., and Hochstrasser, M. (1993) *Nature 366*, 313−319.
12. Zhu, Y., Lambert, K., Corless, C., Copeland, N. G., Gilbert, D. J., Jenkins, N. A., and D'Andrea, A. D. (1997) *J. Biol. Chem. 272*, 51−57.
13. Schofield, J. M., Day, I. N. M., Thompson, R. J., and Edwards, Y. H. (1995) *Dev. Brain Res. 85*, 229−238.
14. Maki, A., Mohammad, R. M., Smith, M., and Al−Katib, A. (1996) *Differentiation 60*, 59−66.
15. Huang, Y., Baker, R. T., and Fischer-Vize, J. A. (1995) *Science 280*, 1828−1831.
16. Chen, Z., and Pickart, C. M. (1990) *J. Biol. Chem. 265*, 21835−21842.
17. Melandri, F., Grenier, L., Plamondon, L., Huskey, W. P., and Stein, R. L. (1996) *Biochemistry 35*, 12893−12900.
18. Pickart, C. M., and Rose, I. A. (1985) *J. Biol. Chem. 260*, 7903−7910.
19. Pickart, C. M., and Rose, I. A. (1986) *J. Biol. Chem. 261*, 10210-1217.
20. Wilkinson, K. D., Cox, M. J., Mayer, A. N., and Frey, T. (1986) *Biochemistry 25*, 6644−6649.

21. Moskovitz, J. (1994) *Biochem. Biophys. Res. Commun. 205*, 354−360.
22. Bizzozero, S. A., Kaiser, A. W., and Dutler, H. (1973) *Eur. J. Biochem. 33*, 292−300.
23. Morrison, J. F., and Walsh, C. T. (1988) *Adv. Enzymol. 61*, 201−301.
24. Szedlacsek, S. E., and Duggleby, R. G. (1995) *Methods Enzymol. 249*, 144−180.
25. Welch, G. R., Somogyi, B., and Damjanovich, S. (1982) *Prog. Biophys. Mol. Biol. 39*, 109−146.
26. Somogyi, B., Welch, G. R., and Damjanovich, S. (1984) *Biochim. Biophys. Acta 768*, 81−112.
27. Gavish, G. (1980) *Phys. Rev. Lett. 44*, 1160−1163.
28. Larsen, C. N., Price, J. S., and Wilkinson, K. D. (1996) *Biochemistry 35*, 6735−6744.
29. Christensen, U., and Ipsen, H. H. (1979) *Biochim. Biophys. Acta 569*, 177−183.
30. Stein, R. L., Viscarello, B., and Wildonger, R. A. (1984) *J. Am. Chem. Soc. 106*, 796−798.
31. Stein, R. L., Strimpler, A. M., Hori, H., and Powers, J. C. (1987) *Biochemistry 26*, 1301−1305.
32. Ng, K., and Rosenberg, A. (1991) *Biophys. Chem. 39*, 57−68.
33. Oh-oka, H., Iwaki, M., and Itoh, S. (1997) *Biochemistry 36*, 9267−9272.
34. Ansari, A., Jones, C. M., Henry, E. R., Hofrichter, J., and Eaton, W. A. (1992) *Science 256*, 1796−1798.
35. Kramers, H. A. (1940) *Physica (Utrecht) 7*, 284−304.
36. Lewis, C. A., and Wofenden, R. (1977) *Biochemistry 16*, 4886−4890.
37. Lewis, C. A., and Wolfenden, R. (1977) *Biochemistry 16*, 4890−4895.
38. Wolfenden, R. (1972) *Acc. Chem. Res. 5*, 10−18.
39. Kahne, D., and Still, W. C. (1988) *J. Am. Chem. Soc. 110*, 7529−7523.
40. Schroder, E., Phillips, C., Garmen, R., Harlos, K., and Crawford, C. (1993) *FEBS Lett. 315*, 38−42.
41. Bendall, M. R., Cartwright, I. L., Clark, P. I., Lowe, G., and Nurse, D. (1977) *Eur. J. Biochem. 79*, 201−209.
42. Jencks, W. P., and Page, M. I. (1972) *Proc. Eighth FEBS Meeting, Amsterdam 29*, 45−58.
43. Page, M. I. (1977) *Angew. Chem., Int. Ed. Engl. 16*, 449−459.
44. Stein, R. L. (1985) *J. Am. Chem. Soc. 107*, 7768−7769.
45. Johnston, S. C., Larsen, C. N., Cook, W. J., Wilkinson, K. D., and Hill, C. P. (1997) *EMBO J. 16*, 3787−3796.

BI9723360